Continuously Tunable Photonic Fractional Hilbert Transformer using Ring Resonators for On-chip Microwave Photonic Signal Processing

Leimeng Zhuang [#1], Willem Beeker [*2], Arne Leinse [*3], René Heideman [*4] and Chris Roeloffzen [#5]

[#]Telecommunication Engineering Group, University of Twente, P. O. Box 217, Enschede 7500AE, The Netherlands
[*]LioniX B.V., P. O. Box 456, Enschede 7500 AL, The Netherlands
l.zhuang@ewi.utwente.nl

***Abstract*—We propose and demonstrate a wideband photonic fractional Hilbert transformer implemented using a ring resonator-based optical all-pass filter. The full programmability of the ring resonators allows variable and arbitrary fractional order of the Hilbert transformer. The implemented all-pass filter performs a good approximation to the ideal Hilbert transform response, and it can be used as a building block to construct on-chip complex microwave photonic signal processors.**

Keywords—fractional Hilbert transformer; optical ring resonator; all-pass filter; microwave photonics; on-chip signal processing;

I. INTRODUCTION

Microwave photonic (MWP) signal processing leverages the advantageous properties of optical devices to realize functionalities performing RF signal processing, so that the constructed systems are commonly associated with the features such as large RF instantaneous bandwidth, RF frequency transparency, light weight, low signal propagation loss, and electromagnetic interference immunity [1], [2]. This technique enables functionalities which are difficult, if not impossible, to realize using only electronics. In the past few years, the advancing of microwave photonics has also exhibited a trend of on-chip realization of various RF signal processing functionalities [3]-[9], enabling on-chip complex MWP signal processors. This improves the system with respect to compactness, robustness, stability, and fabrication cost, especially when the chip is fabricated using CMOS process-compatible equipment. To enrich the applications of MWP signal processing, several recent investigations have been conducted on photonic implementations of a wideband fractional Hilbert transformer (FHT), which is a fundamental operator used for numerous signal processing functionalities in radar, communication, and modern instrumentation systems [10]. However, the previously reported photonic FHTs are all based on bulky systems using either a fiber bragg grating and circulator [11], [12], or a delay-line filter requiring multiple lasers [13], [14], which manifest the lack of tunability and high system complexity/cost, respectively. In this paper, we propose and demonstrate a simple photonic on-chip implementation of a FHT using ring resonator-based optical all-pass filters. The full programmability of the ring resonators allows variable and arbitrary fractional order of the FHT. In addition to that, the waveguide realization of ring resonators allows this FHT to be integrated together with other functional building blocks on a photonic integrated circuit (PIC) to create various system-level functionalities for on-chip MWP signal processors. In Section II the design of a photonic FHT using ring resonator-based optical all-pass filter is described in association with a performance analysis. The characterization of a waveguide realization of the proposed photonic FHT is presented in Section III with the demonstration of RF measurements. In Section IV conclusions are given including several possible applications of the proposed photonic FHT.

II. PHOTONIC IMPLEMENTATION OF FRACTIONAL HILBERT TRANSFORMER

A. Theory of FHT

According to [10], the temporal complex envelope of an output optical signal $y(t)e^{j2\pi f_0 t}$ of a conventional Hilbert transformer (HT) (f_0 is the optical carrier frequency) is given by

$$y(t) = \text{P.V.}\left[\frac{1}{\pi}\int_{-\infty}^{\infty}\frac{x(\tau)}{t-\tau}d\tau\right] = x(t) * \frac{1}{\pi t} \quad (1)$$

where $x(t)$ is the temporal complex envelope of the input optical signal $x(t)e^{j2\pi f_0 t}$ and P.V. means principle value. Thus, the HT can be implemented using a linear optical filter providing a temporal impulse response $h_{FHT}(t)e^{j2\pi f_0 t}$ with an envelope $h_{\text{HT}}(t) = 1/(\pi t)$ and a corresponding frequency response $H_{\text{HT}}(f_{\text{b}}) = -j\text{sgn}(f_{\text{b}})$, where f_{b} is the baseband frequency variable ($f_{\text{b}} = f - f_{\text{o}}$, with f indicating the optical frequency). When a conventional HT is generalized into FHT and the approaches in [15] are used to approximate the ideal $H_{\text{FHT}}(f_{\text{b}})$ using optical filters, the discrete-time version of $H_{\text{FHT}}(f_{\text{b}})$ is defined and is given by

$$H_{\text{FHT}}(\Omega) = |H_{\text{FHT}}(\Omega)|e^{\text{j}\Psi(\Omega)} = \begin{cases} e^{-\text{j}\phi}, & 0 \le \Omega < \pi \\ e^{\text{j}\phi}, & -\pi \le \Omega < 0 \end{cases} \quad (2)$$

where Ω represents the angular frequency normalized to the defined unit delay of the filter, $\phi = \rho \cdot \pi/2$ and ρ indicates the fractional order. This expresses that a FHT is an ideal $\rho \cdot \pi/2$ phase shifter. A FHT becomes the conventional HT $H_{\text{HT}}(\Omega) = -j\text{sgn}(\Omega)$ when $\rho = 1$, and it provides no modification to the input signal when $\rho = 0$ (results in $H_{\text{FHT}}(\Omega) = 1$). By definition, the FHT has its operation bandwidth equal to the defined frequency period. Moreover, the response $H_{\text{FHT}}(\Omega)$ is also periodic with ρ. Since

The research described in this paper is funded by the Dutch Point One R&D Innovation Project: Broadband Satellite Communication Services on High-Speed vehicles.

$H_{\mathrm{FHT}}(\Omega)|_{\rho\pm4} = H_{\mathrm{FHT}}(\Omega)|_{\rho}$ holds, the period of FHT is four. Compute the inverse Fourier transform of $H_{\mathrm{FHT}}(\Omega)$, the corresponding impulse response is given by

$$h_{\mathrm{FHT}}(n) = \begin{cases} \cos(\phi), & n = 0 \\ \sin(\phi)\frac{2sin^2(n\pi/2)}{n\pi}, & n \neq 0 \end{cases} \quad (3)$$

It can be seen that $h_{FHT}(n)$ is zero when n is a nonzero even integer, and its negative taps have opposite values to the corresponding positive taps, forming an anti-symmetric profile with respect to $n = 0$. An illustration of the frequency and impulse response of an ideal HT is depicted in Figure 1.

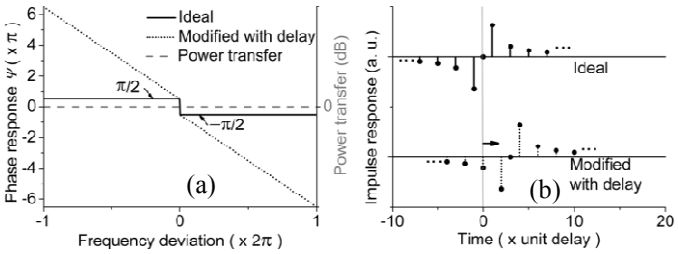

Figure 1. (a) the frequency responses and (b) the corresponding impulse response profile of an ideal and a delay-modified discrete-time HT.

Apparently, an ideal FHT is not realizable in practice, since $h_{\mathrm{FHT}}(n)$ in (3) has infinite length and is non-causal, making FIR and IIR filters inapplicable. To solve this problem, one can approximate the modified specification $H'_{\mathrm{FHT}}(\Omega)$ instead, which is the frequency response by cascading ideal FHT and a pure delay length. $H'_{\mathrm{FHT}}(\Omega)$ is defined by

$$H'_{\mathrm{FHT}}(\Omega) = H_{\mathrm{FHT}}(\Omega)e^{-jn_0\Omega} = \begin{cases} e^{-jn_0\Omega}e^{-j\phi} & 0 \le \Omega < \pi \\ e^{-jn_0\Omega}e^{j\phi} & -\pi \le \Omega < 0 \end{cases} \quad (4)$$

where n_0 is a prescribed delay, resulting in a time shift of the impulse response as illustrated in Figure 1(b). Once an FIR or IIR filter $G(\Omega)$ is designed, we use the following formula to obtain the designed result $\hat{H}_{\mathrm{FHT}}(\Omega)$ of the FHT:

$$\hat{H}_{\mathrm{FHT}}(\Omega) = G(\Omega)e^{jn_0\Omega} \quad (5)$$

Then, a signal passing through an optical filter described by $G(\Omega)$ experiences the same effect as it passes through a cascade system of a pure delay length $e^{-jn_0\Omega}$ and a designed FHT with frequency response $\hat{H}_{\mathrm{FHT}}(\Omega)$.

B. All-pass filter approach

To approximate $H'_{\mathrm{FHT}}(\Omega)$ in (4) the well-documented FIR and IIR design approaches can be used. Among them one option is to use an all-pass filter [15], since the amplitude response of $H'_{\mathrm{FHT}}(\Omega)$ is equal to unity for all frequencies. Using the general z-transform description for discrete-time filter design, an *N*th order all-pass filter $G_N(z)$ is given by

$$G_N(z) = \frac{a_N + a_{N-1}Z^{-1} + \cdots + a_1 z^{-N+1} + Z^{-N}}{1 + a_1 z^{-1} + \cdots + a_{N-1}z^{-N+1} + a_N z^{-N}} \quad (6)$$

If $\varphi_G(\Omega)$ is used to denote the phase response of all-pass filter $G_N(z)$, then one should design the all-pass filter $G_N(z)$ such that the $\varphi_G(\Omega)$ approximates the prescribed phase response in (4). Using the design method described in [16], the optimal filter coefficients $a_1, \cdots, a_N$ can be determined in the least squares error sense.

C. Optical ring resonator

An ideal lossless optical ring resonator (ORR) is a first-order all-pass filter, and a cascade of ORRs can be used in practice to implement $G_N(z)$ in (6) [15]. A schematic of an ORR in waveguide implementation is depicted in Figure 2 with an illustration of the profile of its impulse response. The corresponding z-transform of the ORR is given by

$$H(z) = \frac{c + rZ^{-1}}{1 + crZ^{-1}} \quad (7)$$

where $c = \sqrt{1-\kappa}$ with κ being the power coupling ratio, and r indicates the roundtrip amplitude transmission coefficient determined by the roundtrip loss. In practice an additional phase shift θ can be applied in the ring path, then z^{-1} becomes $z^{-1}e^{-j\theta}$ which performs a frequency shift of the frequency response of the ORR by $\Delta f = \Delta f_{\mathrm{FSR}}\theta/2\pi$ with Δf_{FSR} being the free spectral range (FSR) of the ORR. Moreover, a Mach-Zehnder interferometer (MZI) is structured to close the ring path, which serves as a practical tunable power coupler when a variable optical phase difference is introduced between the two arms.

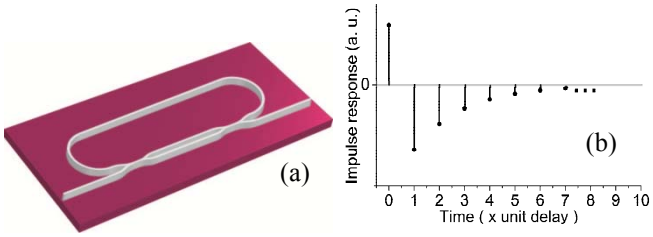

Figure 2. (a) schematic of waveguide implementation of an ORR and (b) profile of the impulse response of an ORR

According to (7) the magnitude and phase response of an actual ORR can be derived and given by

$$|H(\Omega)| = \sqrt{\frac{c^2 + r^2 - 2cr\cos(\Omega)}{1 + cr^2 - 2cr\cos(\Omega)}} \quad (8)$$

and

$$\Psi(\Omega) = \arctan\left[\frac{\frac{r}{c}\sin(\Omega)}{1 - \frac{r}{c}\cos(\Omega)}\right] - \left[\frac{cr\sin(\Omega)}{1 - cr\cos(\Omega)}\right] \quad (9)$$

respectively. By definition an ORR has a fixed phase shift of 2π across one FSR. Using this as a condition to (4), one can obtain the relation

$$n_0 = 1 - \frac{\rho}{2} \quad (10)$$

Then, the purpose is to approximate $H'_{\mathrm{FHT}}(\Omega)$ in (4) by applying the corresponding optimal filter coefficient $c = \sqrt{1-\kappa}$, which one can vary by means of the tunable power coupler. Figure 3 depicts the frequency responses of the ORR optimized to fit $H'_{\mathrm{FHT}}(\Omega)$ for different fractional order ρ, where $r = 0.97$ is used corresponding to roundtrip loss of 0.12 dB. Due to the fact that an ORR can only provide an approximation to a linear phase response as indicated in (9), the operation bandwidth of the ORR-based FHT is then determined according to the defined phase ripple tolerance

requirement. This relation is illustrated in Figure 4 for different values of ρ, with the operation bandwidth normalized to the FSR of the ORR.

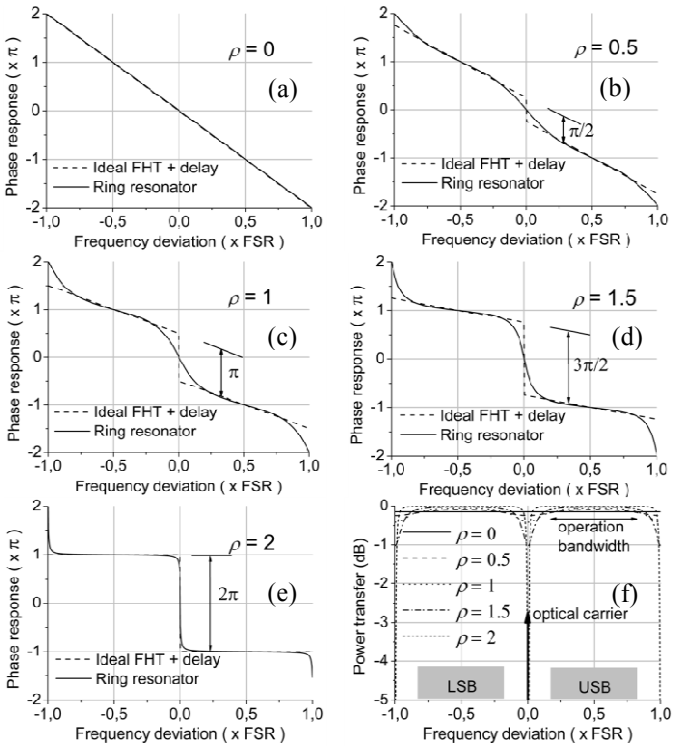

Figure 3. Phase responses of an ORR optimized to the target FHT response for different fractional orders (a) $\rho = 0$, (b) $\rho = 0.5$, (c) $\rho = 1$, (d) $\rho = 1.5$, (e) $\rho = 2$, and (f) the corresponding power transfers of the ORR ($r = 0.97$).

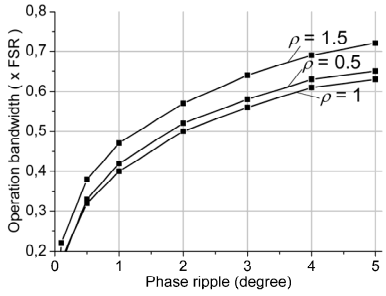

Figure 4. Operation bandwidth of ORR-based FHT related to phase ripple tolerance requirement.

Furthermore, the power transfer of the ORR depicted in Figure 3(f) demonstrates a strong notch effect for $\rho = 2$ corresponding to a high-Q state of the ORR. This will result in strong optical carrier suppression. However, in the scenario of a system using direction detection, the presence of optical carrier is required to recover the signals modulated on the light. To solve this problem, the desired FHT can be approximated using a cascade of multiple ORRs instead of a single ORR. Being a linear system, a cascade of *N* ORRs can be described by

$$H_c(\Omega) = \sum_{n=1}^{N} H_n(\Omega) = \prod_{n=1}^{N} |H_n(\Omega)| \, e^{\sum_{n=1}^{N} -j\Psi_n(\Omega)} \quad (11)$$

Thus, a desired FHT performing a fractional order ρ can be obtained by letting each ORR in the cascade provide a division of ρ, so that the high-Q state of the ORRs can be avoided, which reduces the notch effect at the optical carrier frequency. Moreover, the lower the waveguide propagation loss is, the lower the power suppression of the FHT results. For a comparison, the frequency responses of a FHT using one ORR and another FHT using two cascaded ORRs are depicted in Figure 5, with both having $\rho = 2$ and $r = 0.97$.

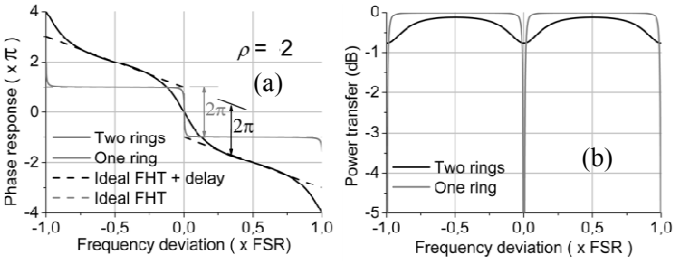

Figure 5. (a) phase response and (b) power transfer of a FHT using one ORR and another FHT using two cascaded ORR ($r = 0.97$).

III. DEVICE REALIZATION AND CHARACTERIZATION

To demonstrate the proposed photonic on-chip FHT, a number of ORRs were fabricated in TriPleX^{TM} waveguide technology, a proprietary technology of LioniX B.V., which can be fabricated using CMOS process-compatible equipment [17]. In this technology a waveguide geometry has been characterized showing a very low propagation loss of 0.1 dB/cm and simultaneously a small bend radius of 70 μm [18], which enables the realization of low loss, compact on-chip MWP signal processors. The ORRs used to characterize the FHT functionality is designed to have a layout as depicted in Figure 2(a): a racetrack-shaped ring connected to a MZI. The ORR has a roundtrip length of 13 mm and a group index of 1.55 resulting in a FSR of 15 GHz. Moreover, two optical phase tuning elements are implemented in the ring path and one arm of the MZI by means of the thermo-optical tuning mechanism using resistor-based heaters. This allows the programmability of the resonance frequency (optical carrier frequency) and the power coupling ratio κ of the ORR. The measurement setup is depicted in Figure 6. The light from a CW laser (EM4253-80-057) is modulated using a Mach Zehnder modulator (Avanex PowerLog FA-20). The modulating RF signal is generated by an vector network analyzer (Agilent NA5230A PNA-L). After performing optical detection (Emcore_17dBm_30Gb/s) the output RF signal is measured by the vector network analyzer to characterize the frequency response of the photonic FHT. For the measurement, the reference was defined by calibrating the S_{21} response to the state where the ORR is decoupled ($\kappa = 0$). This removes the effects of the other components in the setup. Then, by setting the optical carrier frequency aligned with the resonance frequency of the ORR and varying κ, different RF phase shift introduced by the ORR can be measured. Figure 7(a) depicts the S_{21} phase measurement results with the fittings of the design target according to (4). In Figure 7(b) the corresponding FHT phase shifts are shown by removing the linear slope of the delay n_0 as explained in (5). Here, a

wideband FHT is demonstrated with operation frequency span from 3 to 12 GHz and overall phase ripple smaller than 5 degree. Although not shown in this paper, the measured power transfer of the FHT is close to flat across the defined bandwidth with less than 1 dB deviation at the band edge, which agrees with the simulations in Figure 3(f).

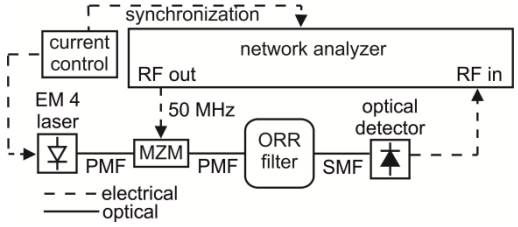

Figure 6. Illustration of measurement setup

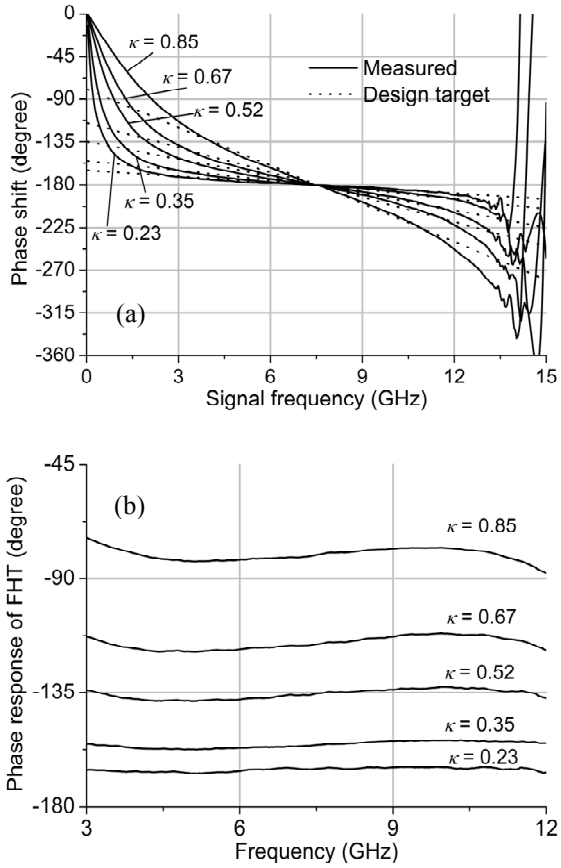

Figure 7. (a) measured different RF phase shifts of the ORR by varying the power coupling ratio κ, and the fittings of the design target; (b) corresponding FHT phase shift by removing the linear slope of delay n_0 for a wideband span from 3 to 12 GHz.

IV Conclusion

In this paper a simple photonic on-chip implementation of wideband FHT is proposed and demonstrated. The FHT is based on an optical all-pass filter using ORRs. The full programmability of the ORRs allows variable and arbitrary fractional order of the FHT, and the waveguide realization allows the device to be integrated with other functional building blocks on a PIC to create various system-level functionalities for on-chip MWP signal processors. The realized device demonstrated a RF bandwidth from 3 to 12 GHz with phase ripple smaller than 5 degree, however, this can be upscaled by using ORRs with larger FSRs. To date, numerous applications of photonic FHTs have been considered, such as optical single sideband generation, instantaneous frequency measurement, wideband vector modulator and quadrature filter to name a few. In addition to those, the proposed photonic on-chip FHT could also be used together with a dual(multi)-wavelength laser for simultaneous generation of RF I/Q signals featuring a wide RF frequency tunability. However, further investigations are still needed to explore its usage.

References

[1] J. Capmany and D. Novak, "Microwave photonics combines two worlds," *Nat. Photonics* **1**(6), 319-330 (2007).

[2] A. Seeds, "Microwave photonics," *IEEE Trans. Microwave Theory Tech.* **50**(3), 877-887 (2002).

[3] F. Liu et al., "Compact optical temporal differentiator based on silicon microring resonator," *Opt. Express* **16**(20), 15880-15886 (2008).

[4] M. Ferrera et al., "On-chip CMOS-compatible all-optical integrator," *Nat. Commun.* **1**(29) (2010).

[5] A. Meijerink et al., "Novel ring resonator-based integrated photonic beamformer for broadband phased-array antennas-Part I: design and performance analysis," *J. Lightwave Technol.*, **28**(1), 3-18 (2010).

[6] L.Zhuang et al., "Novel ring resonator-based integrated photonic beamformer for broadband phased-array antennas-Part II: experimental prototype," *J. lightwave Technol.*, **28**(1), 19-31 (2010).

[7] D. Marpaung et al., "A photonic chip based frequency discriminator for a high performance microwave photonic link," *Opt. Express*, **18**(26), 27359-27370 (2010).

[8] D. Marpaung et al., "Impulse radio ultrawideband pulse shaper based on a programmable photonic chip frequency discriminator," *Opt. Express*, **19**(25), 24839-24848 (2011).

[9] M. Burla et al., "On-chip CMOS compatible reconfigurable optical delay line with separate carrier tuning for microwave photonic signal processing," *Opt. Express*, **19**(22), 21476-21484 (2011).

[10] S. L. Hahn, *Transforms and Applications Handbook*, A. D. Poularikas, Ed., 3rd. Boca Raton, FL: CRC Press, 2010.

[11] M. H. Asghari and J. Azaña, "All-optical hilbert transformer based on a single phase-shifted fiber bragg grating:design and analysis," *Opt. Letters*, **34**(3), 334-336 (2009)

[12] M. Li and J. Yao, "All-fiber temporal photonic fractional hilbert transformer based on a directly designed fiber bragg grating," *Opt. Letters*, **35**(2), 223-225 (2010).

[13] H. Emami et al., "Wideband RF photonic in-phase and quadrature-phase generation," *Opt. Letters*, **33**(2), 98-100 (2008).

[14] Z. Li et al., "A continously tunable microwave fractional hilbert transformer based on a photonic microwave delay-line filter using a polarization modular," *Opt. Letters*, **23**(22), 1694-1696 (2011).

[15] C. K. Madsen and J. H. Zhao, *Optical filter design and analysis*, New York: Wiley, 1999.

[16] M. Lang and T. I. Laakso, "Simple and robust method for the design of allpass filters using least squares phase error criterion," *IEEE Trans. Circuits Syst. II*, Vol. 41, 40-48 (1994).

[17] R. G. Heideman et al., "Large-scale integrated optics using TriPleX waveguide technology:from UV to IR," *Proc. SPIC 7221*, 72210R-1-72210R-15 (2009).

[18] L. Zhuang et al., "Low-loss, high-index-contrast Si3N4/SiO2 optical waveguides for optical delay lines in microwave photonics signal processing," *Opt. Express*, **19**(23), 23162-23170 (2011).